Geophysical Journal International

Geophys. J. Int. (2012) **190,** 1311–1324 doi: 10.1111/j.1365-246X.2012.05580.x

3-D lithospheric structure and regional/residual Bouguer anomalies in the Arabia–Eurasia collision (Iran)

I. Jiménez-Munt, M. Fernàndez, E. Saura, J. Vergés and D. Garcia-Castellanos

Group of Dynamics of the Lithosphere (GDL), Institute of Earth Sciences 'Jaume Almera', ICTJA-CSIC, Solé i Sabarís s/n, 08028 *Barcelona, Spain. E-mail: ivone@ictja.csic.es*

Accepted 2012 June 15. Received 2012 May 29; in original form 2012 January 17

SUMMARY

The aim of this work is to propose a first-order estimate of the crustal and lithospheric mantle geometry of the Arabia–Eurasia collision zone and to separate the measured Bouguer anomaly into its regional and local components. The crustal and lithospheric mantle structure is calculated from the geoid height and elevation data combined with thermal analysis. Our results show that Moho depth varies from ∼42 km at the Mesopotamian–Persian Gulf foreland basin to ∼60 km below the High Zagros. The lithosphere is thicker beneath the foreland basin (∼200 km) and thinner underneath the High Zagros and Central Iran (∼140 km). Most of this lithospheric mantle thinning is accommodated under the Zagros mountain belt coinciding with the suture between two different mantle domains on the Sanandaj–Sirjan Zone. The regional gravity field is obtained by calculating the gravimetric response of the 3-D crustal and lithospheric mantle structure obtained by combining elevation and geoid data. The calculated regional Bouguer anomaly differs noticeably from those obtained by filtering or just isostatic methods. The residual gravity anomaly, obtained by subtraction of the regional components to the measured field, is analyzed in terms of the dominating upper crustal structures. Deep basins and areas with salt deposits are characterized by negative values (∼−20 mGal), whereas the positive values are related to igneous and ophiolite complexes and shallow basement depths (∼20 mGal).

Key words: Gravity anomalies and Earth structure; Continental tectonics: compressional; Dynamics: gravity and tectonics; Crustal structure.

INTRODUCTION

The Zagros mountain belt and its foreland basin (Fig. 1) are an area with a huge potential in natural resources (mainly oil and gas). One of the main targets in oil exploration is to characterize the structure of the sedimentary cover and the topography of the crystalline basement. Moreover, oil generation is very sensitive to the heat stored by the source rock and therefore to the tectonic evolution of the entire lithosphere. During the last decade the Zagros fold-and-thrust belt and its foreland basin have been the target of numerous geophysical surveys to unravel the crustal and lithospheric structure of the region. These studies include the analysis of receiver functions in single seismic stations, which provides 1-D lithospheric models (e.g. Doloei & Roberts 2003; Gök *et al.* 2008; Nasrabadi *et al.* 2008; and references on Fig. 2), and over 2-D transects across the Zagros mountain belt (e.g. Paul *et al.* 2006, 2010). Regional tomography models have been also developed to image the upper mantle structure over the whole region (e.g. Al-Damegh *et al.* 2004; Alinaghi *et al.* 2007; Manaman *et al.* 2011). All these studies show a variable resolution depending on the particular area subject to analysis and the method used. A regional study using a homogeneous methodology giving a reliable and detailed image of the crust and lithospheric mantle variations still lacks.

Gravity modelling when combined with additional techniques and data sets is a powerful tool to gain knowledge in the shallow and deep structure of large regions. In particular, the Bouguer gravity anomaly can be separated in its regional and long wavelength component, related to the contribution of deep-seated lateral density variations, and its local and short wavelength component caused by shallow geological features as sedimentary basins, basement topography, major salt intrusions and igneous and ophiolite complexes.

Several methodologies have been applied by different authors to obtain the residual gravity anomaly for Iran (e.g. Dehghani & Makris 1984; Snyder & Barazangi 1986; Kiamehr 2006; Ardalan *et al.* 2011), which provided results with variations exceeding 20 mGal among them. One of the main problems in computing the residual gravity anomaly in the Zagros region is the scarcity of geophysical data to add constraints to this calculation. Accordingly, the best way to validate the calculated Bouguer residual anomaly is by comparing the obtained field with surface geology.

The aim of this work is to provide a first-order estimate of the crustal and lithospheric mantle geometries of the Arabia–Eurasia

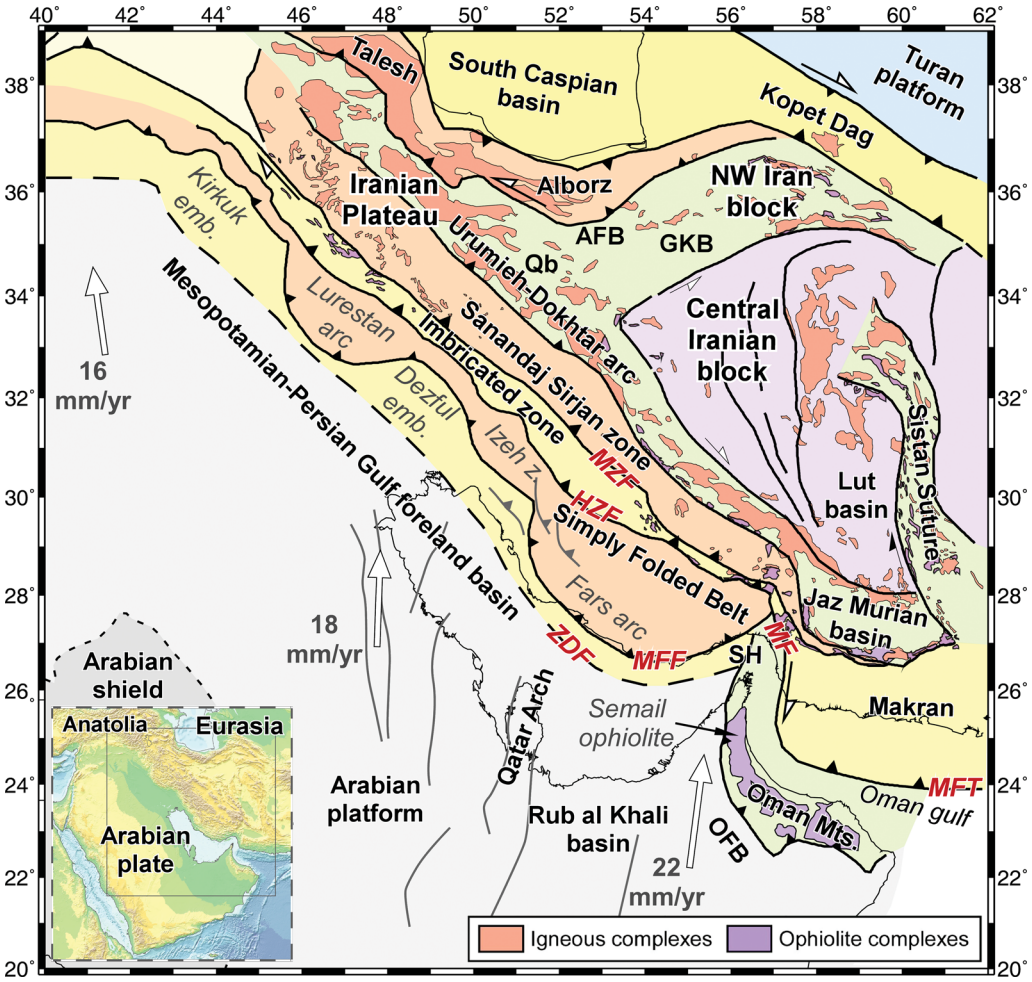

Figure 1. Structural map showing the main tectonic units of the Zagros Mountains and adjacent areas, including major igneous and ophiolitic complexes. The colours assigned to the different tectonic units are not related to age or lithology but are used to highlight their limits. White arrows correspond to the relative plate velocities of the Arabian plate with respect to a fixed Eurasian plate. ZDF = Zagros deformation front; MFF = Mountain Front Flexure; HZF = High Zagros Fault; MZF = Main Zagros Fault; Qb = Qom basin; GKB = Great Kabir basin; and AFB = Alborz foredeep basin; OFB = Oman foreland basin; SH = Strait of Hormuz; MF = Minab Fault; MFT = Makran frontal thrust.

collision zone and to separate the measured Bouguer anomaly into its regional and local components. In addition to the crustal and lithospheric thickness maps, this study also brings new insights on the geology of the Zagros mountain belt and on the large-scale geodynamics of this segment of the Arabia–Eurasia collision.

GEOLOGICAL SETTING

The long-lived convergence between Arabia and Eurasia since Late Cretaceous times resulted in subsequent collision stages between Arabia and smaller continental blocks resulting from the break-up of Gondwana until the final closure of the Neo-Tethys Ocean. The Zagros-Oman-Makran orogenic system was built along the north-eastern margin of Arabia whereas the Alborz and Kopet Dag developed along the contacts between Iran and the Caspian Sea and Eurasia, respectively. This long geodynamic evolution became in a complex geological structure characterized by important lateral variations in age, composition and tectonic style over this large region (Golonka 2004; Hatzfeld & Molnar 2010).

The opening of the Red Sea at the end of Oligocene times separated Arabia from Africa producing the uplift of the Arabian Shield, which exposed the Precambrian crystalline basement. Major N-S trending faults define the SE boundary of the shield and form the Qatar Arch and the Rub al Khali Basin (Fig. 1). The Arabian Plate consists of a late Proterozoic basement overlain by a thick Phanerozoic cover, including the Paleozoic-Mesozoic pre-orogenic and the Tertiary synorogenic successions (Konert *et al.* 2001).

The Arabian Plate flexed down during the evolution of the Zagros orogenic system forming the Mesopotamian foreland basin and the Persian Gulf in front of the Zagros mountain belt and of its SE continuation in Oman. The early foreland depositional sequences are exposed in the Lurestan arc, with a thickness of 1.6 km deposited from the latest Cretaceous to the early Eocene times (Saura *et al.* 2011). The youngest foreland basin to the south-west of the Zagros Front shows more than 5 km of syntectonic deposits (Fars Group) that wedge and thin westwards (Konert *et al.* 2001).

The NW-SE-trending Zagros orogenic system is divided in four parallel structural domains (Fig. 1): (1) the Simply Folded Belt bounded by the Mountain Front Flexure (MFF; Falcon 1961; Berberian 1995; Sepehr & Cosgrove 2004; Emami *et al.* 2010), (2) the Imbricate Zone (also called High Zagros Thrust Belt or Crush Zone), limited by the High Zagros Fault (HZF, Berberian 1995), (3)

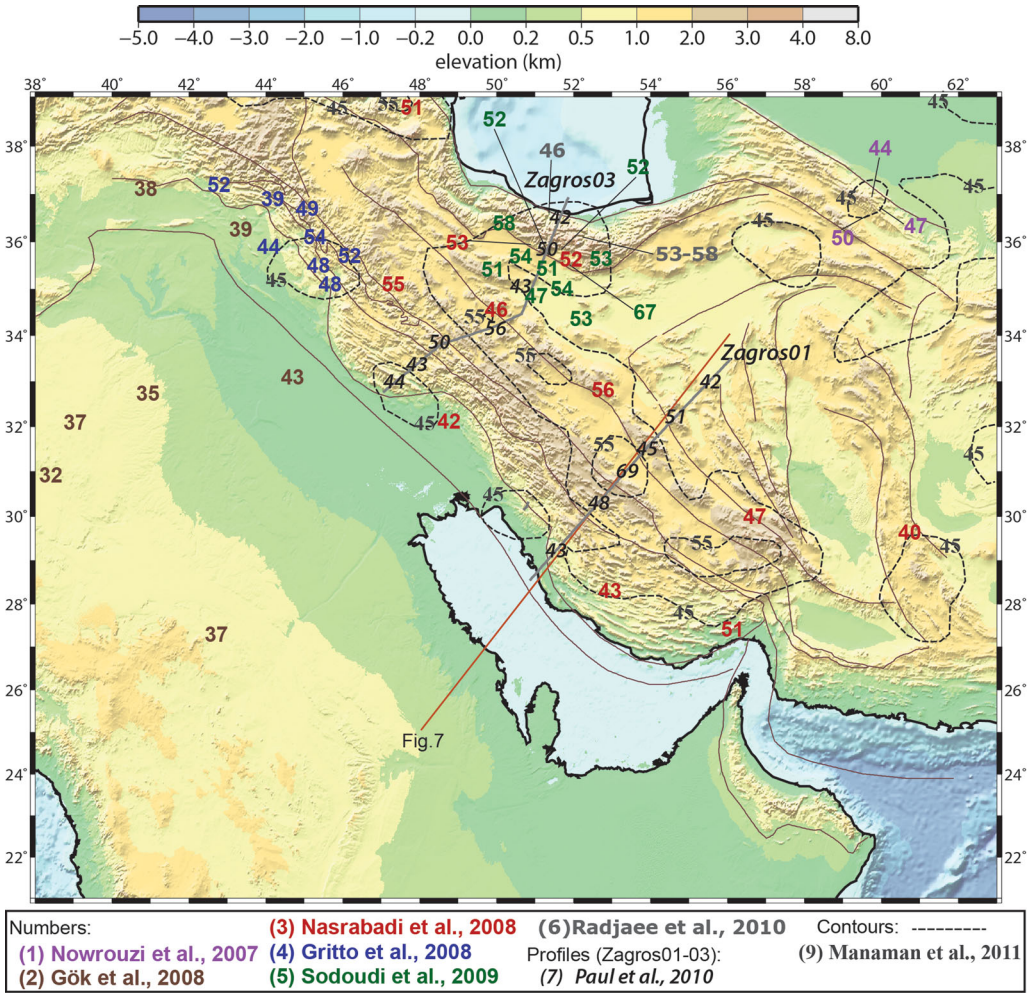

Figure 2. Topographic map (colour pattern) from ETOPO1 (Amante & Eakins 2009) and crustal thicknesses (numbers) obtained from other studies, see colours for references. Results from receiver function on the Arabian plate (Gök *et al.* 2008), along Zagros Mountains (Nasrabadi *et al.* 2008; Gritto *et al.* 2008), on Alborz and its forelands (Nasrabadi *et al.* 2008; Sodoudi *et al.* 2009; Radjaee *et al.* 2010) and on Kopet Dag (Nowrouzi *et al.* 2007). Results over 2-D transects across the Zagros fold-and-thrust belt (Zagros01 and Zagros03, Paul *et al.* 2010). And the black dashed lines are the results from regional tomographic models (Manaman *et al.* 2011). Grey lines correspond to the main structural boundaries (see Fig. 1). Orange line corresponds to the profile on Fig. 7.

the metamorphic and magmatic Sanandaj–Sirjan Zone separated from previous unit by the Main Zagros Fault (MZF) (e.g. Falcon 1967; Stocklin 1968) and (4) the Urumieh–Dokhtar Magmatic Arc.

In the Simply Folded Belt, the sedimentary cover of the Arabian Plate is detached from the Pre-Cambrian basement and the syntectonic deposits are only preserved in the core of the synclines. The sinuous trace of MFF delineating the Kirkuk Embayment, the Lurestan arc, the Dezful Embayment and the Fars arc (Fig. 1) is apparently related to the distribution of the Hormuz salt, acting as a decoupling level (Kent 1979; Bahroudi & Koyi 2003; Casciello *et al.* 2009). The Imbricated Zone (IZ) is a highly deformed terrain, formed by a pile of thrust sheets including, from bottom to top, the distal part of the Arabian Margin, ophiolite complexes, volcanic arc complexes, and slices from the metamorphic Sanandaj–Sirjan zone (Braud 1970; Nemati & Yassaghi 2010). These thrust sheets were carried to the SW above the Kermanshah thrust (Vergés *et al.* 2011) (Fig. 1).

In the hanging wall of the MZF, the Sanandaj–Sirjan Zone is a ∼150–200 km-wide belt, NW-SE trending thrusts involving sedimentary and metamorphic Paleozoic to Mesozoic rocks (Alavi 1994; Masoudi 1997), intruded by Jurassic to early Eocene calc-alkaline magmatic rocks and middle Eocene gabbros (e.g. Valizadeh & Cantagrel 1975; Berberian & Berberian 1981; Leterrier 1985; Braud 1987; Masoudi 1997; Baharifar *et al.* 2004) (Fig. 1). NE of this unit, the Tertiary Urumieh Doktar magmatic arc defines a 50–100 km-wide belt interpreted as an Andean-type magmatic arc formed on the Iranian continental crust associated to the northwards subduction of the Neo-Tethys Ocean (e.g. Bernard *et al.* 1979; Martel-Jentin *et al.* 1979; Berberian *et al.* 1982; Bina *et al.* 1986, Alavi 1994).

The SE continuations of the Zagros orogenic system are the Oman Mountains and the Makran accretionary prism (Fig. 1). The Oman foreland basin infill defines a narrow belt (100 km-wide) with a maximum calculated thickness of about 7 km (Ravaut *et al.* 1997). The Oman Mountains define an arcuate geometry opposed to the SE termination of the Fars Arc confining a very thick foreland sedimentary succession deposited in front of the Zagros and Oman fold-and-thrust belts (Jahani *et al.* 2009). The most distinctive of the Oman Mountains is the large Semail Ophiolite nappe and its metamorphic sole including high-pressure rocks overriding the Arabian platform deposits (Allemann & Peters 1972, Stoneley 1975).

Separated from the Oman Mountains by the Oman Gulf, the Makran accretionary prism shows a relict accretionary prism onshore of middle-upper Miocene age (e.g. Burg *et al.* 2008) and a younger active system developed during the late Miocene-Pliocene offshore (e.g. Ellouz-Zimmermann *et al.* 2007). North of this belt, the Jaz Murian basin is considered the back-arc basin related to the Makran subduction zone, filled with Cenozoic deposits (McCall & Kidd 1982; Glennie *et al.* 1990).

The Alborz Mountains, with topography between 3 and 5 km (Fig. 2), define a large anticlinorium cored by Precambrian basement rocks that are overlain by about 5 km of Phanerozoic sediments (e.g. Ballato *et al.* 2011). The Kopet Dag Mountains are located to the east of the Alborz Range, constituting the north-eastern border of the Arabia–Eurasia collision zone. The Kopet Dag is constituted by Hercynian metamorphic basement covered by about 10 km of Mesozoic-Tertiary sediments (mostly carbonates) folded into long linear NW-SE trending folds (Berberian & Berberian 1981).

A large endorheic basin shapes the northern Central Iran, which is surrounded by the NW Iran block, by the Central Iran block, by the Urumieh-Doktar arc and by the Alborz Mountains (Fig. 1). Three sub-basins can be differentiated: the Great Kabir basin filled by ∼5 km of alternate Tertiary gypsum, limestone and salt, with frequent diapiric features (Jackson *et al.* 1990); the Qom basin containing a maximum thickness of ∼12 km of Tertiary sediments (Morley *et al.* 2009); and the Alborz foreland basin with ∼7.5 km of Tertiary deposits (Ballato *et al.* 2011).

To the north of the Alborz mountain ranges, the South Caspian Basin is characterised by a sedimentary thickness of 20–25 km (Glumov *et al.* 2004) deposited on top of a ∼10 km thick crystalline crust, which have often been interpreted as having an oceanic affinity (Motavalli-Anbaran *et al.* 2011 and references therein). To the north-east of the Kopet Dag the Turan Platform represents Eurasia (e.g. Motavalli-Anbaran *et al.* 2011).

METHOD

The methodology used in our analysis consists of two steps:

(1) In the first step we calculate the depth to Moho and depth to base of the lithosphere by means of fitting elevation and geoid anomaly data combined with thermal analysis. The method used in this first step has already been applied in the Gibraltar Arc System and Atlas Mountains and it is described in Fullea *et al.* (2007). It assumes local isostasy and a crustal density increasing linearly with depth between predefined values at surface and at the base of the crust. The density of the lithosphere mantle is considered to be temperature dependent. The geoid anomalies are calculated relative to a reference lithospheric column. This reference column serves to calibrate the zero level for the geoid anomalies, and must be selected in such way that physically meaningful results are obtained in our lithospheric model (see Fullea *et al.* 2007 for details). In this study, the reference column for geoid anomaly calculations has been chosen in order to fit the crustal thicknesses obtained from previous studies (Fig. 2). We compare and discuss the obtained lithosphere structure with available data.

(2) In the second step we calculate the 3-D Bouguer gravity anomaly associated with this lithosphere structure that by definition will correspond to the regional Bouguer anomaly. The residual gravity anomaly is obtained by subtracting from the measured Bouguer anomaly the calculated regional field.

In this study we have considered a crustal density varying from 2720 kg m^{-3} at surface to 2960 kg m^{-3} at Moho depth, which results in an average crustal density of 2840 kg m^{-3}. In the results section, the obtained lithosphere structure and residual Bouguer anomaly is discussed in relation to the considered crustal density values. The lithospheric mantle density is $\rho_m = \rho_a[1-\alpha(T(z)-T_a)]$, where ρ_a is the density of the asthenosphere (3200 kg m^{-3}), α is the thermal expansion coefficient (3.5×10^{-5} K^{-1}), and T_a is the temperature at the base of the lithosphere (1300 °C). Sea water density is 1031 kg m^{-3}. The thermal conductivity is 3.0 W km^{-1} for the crust and 3.2 W km^{-1} for the lithospheric mantle. The average radiogenic crustal heat production is 0.7 μW m^{-3} (Vilà *et al.* 2010) and null for the lithospheric mantle.

Traditionally the regional/residual Bouguer anomaly separation is achieved by calculating a regional Bouguer gravity field, usually by fitting a low-degree polynomial surface or by applying a low-pass filter to the observed Bouguer gravity anomaly. The resulting regional field by any of these methods is intimately related to the measured field and therefore to the data coverage. An alternative method to calculate the regional gravity component is by assuming that the topographic relief is isostatically compensated. In this way, the resulting regional gravity field is independent on the measured one and reflects more closely the deep structure of the region subjected to study.

We will compare the resulting regional and residual gravity anomalies from our proposed method (combining elevation and geoid data) with these three other methodologies:

(1) Filter: The regional gravity anomaly is calculated by filtering the measured Bouguer anomaly using a Gaussian boxcar filter with a wavelength of 500 km, as proposed in GETECH datafile report.

(2) Crustal isostasy: A crustal model is obtained assuming the Airy hypothesis, where topography is fully compensated by crustal thickness variations. We assume average densities for the crust and lithospheric mantle of 2840 and 3250 kg m^{-3}, respectively.

(3) Lithosphere isostasy: The lithosphere structure is obtained assuming lithosphere isostasy under the additional assumption of pure shear deformation. Therefore, elevation is locally compensated by the crust and the lithospheric mantle, and the ratio between crust and lithosphere mantle thickness is constant everywhere. The averaged densities are 2840 kg m^{-3} for the crust, 3250 kg m^{-3} for the lithospheric mantle and 3200 kg m^{-3} for the asthenosphere. In both crustal and lithosphere isostasy approaches we use a reference column consisting of 38 km thick crust and a total lithospheric thickness of 150 km, which results in an elevation of 0 m above sea level. The regional gravity field is calculated from the resulting lithosphere structures.

DATA

Topography (Fig. 2) is obtained from the ETOPO1 database (Amante & Eakins 2009). The most remarkable feature is the high topography (3500–4000 m) along the Zagros mountain belt, with maximum values in the IZ, extending to the NW into Anatolia. The Iranian Plateau, at the north-east of the Zagros mountain belt, reaches elevations between 700 and 1500 m. The Iranian Plateau is limited by the Alborz Mountains with elevations above 3000 m. The Arabian Plate elevation decreases towards NE from highs of ∼1000 m in the Arabian shield to less than 200 m in the Mesopotamian Foreland and −50 m in the Persian Gulf. To minimize the topographic contribution supported by flexural strength and to avoid unrealistic lateral variations of the Moho and LAB depths we have filtered the elevation using a Gaussian filter of 100

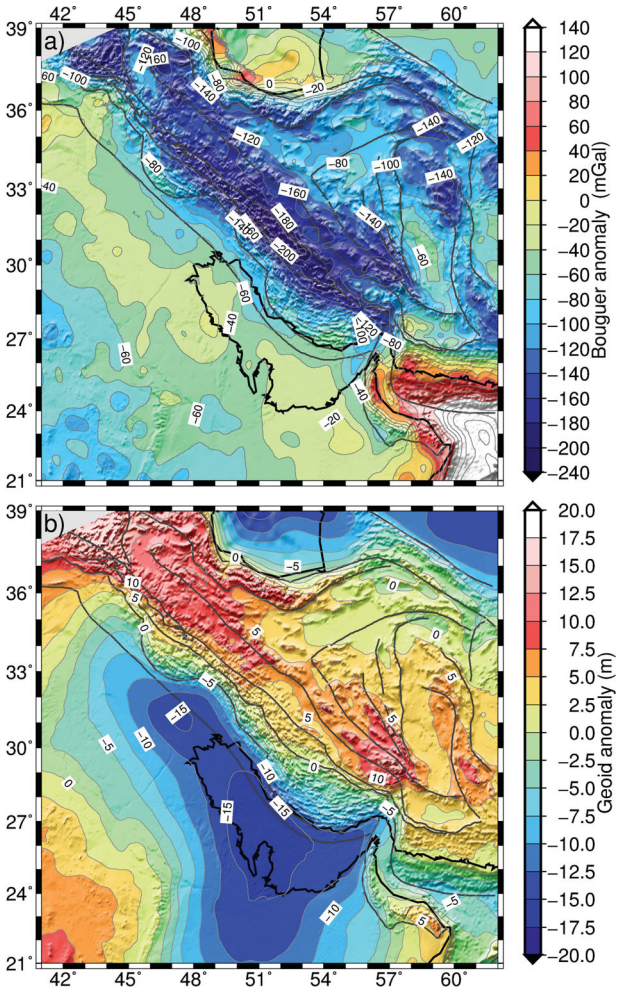

Figure 3. (a) Bouguer anomaly (contours every 20 mGal) from GETECH (http://www.getech.com) in Iran and for the rest of the region is calculated applying the complete Bouguer correction to free air satellite data (Sandwell & Smith 1997). (b) Geoid height (contours every 2.5 m) from EGM2008 global model (Pavlis *et al.* 2008). In order to avoid effects of sublithospheric density variations on the geoid, we have removed the geoid signature corresponding to the lower spherical harmonics until degree and order 9. Shading indicates elevation.

km wavelength prior to the calculations of the crustal and lithosphere thicknesses.

The geoid height is taken from EGM2008 global model (Pavlis *et al.* 2008), which includes spherical harmonic coefficients up to degree and order 2190. In order to avoid effects of sublithospheric density variations, which are out the scope of this work, we have removed the geoid signature corresponding to the lower spherical harmonics. The wavelengths >4000 km (i.e. degrees 2–8) have therefore been removed from the complete geoid to retain the effects of density anomalies shallower than ∼400 km depth (Bowin 2000). We discuss in the results section the effect of removing higher degrees on the geoid. The obtained geoid anomaly (Fig. 3b) shows an amplitude exceeding 30 m. Maximum values are located in the Anatolian Plateau and extend along the Zagros and Alborz mountains. Minimum values are on the Persian Gulf and south-east Arabian Plate, Caspian Sea and north-east on the Turan platform. The Mesopotamian Basin is characterised by anomalies between −8 and −15 m and on the Persian Gulf the geoid reaches values lower than −16 m. Over the Zagros and Central Iran the anomalies range between 4 and 12 m. Lower values, between −2 and 2 m, are measured on the NW Iran block.

The Bouguer gravity anomaly for Iran comes from GETECH (http://www.getech.com), while for the rest of the region it has been calculated applying the complete Bouguer correction to free air satellite data (Sandwell & Smith 1997) using the FA2BOUG code (Fullea *et al.* 2008) with a reduction density of 2670 kg m^{-3}. The Bouguer anomaly (Fig. 3a) along the Zagros mountain belt shows minimum values up to ∼−220 mGal striking parallel to the Zagros Main Thrust and indicating the presence of a crustal root. At the Central Iranian Blocks the gravity field achieves values between −120 and −70 mGal, suggesting a thinner crust beneath. The gravity increases towards the Caspian Sea in the northern side of Alborz Mountains reaching values up to 30 mGal. From the High Zagros Thrust towards SW the Bouguer anomaly increases reaching values between −50 and −20 mGal in the Mesopotamian–Persian Gulf Foreland basin and decreasing again towards the Arabian Shield up to ∼−100 mGal. A sharp gradient, parallel to the NE Persian Gulf coast, marks the transition to the Zagros mountain belt.

RESULTS AND DISCUSSION

In this section we summarize and compare the obtained results with available geological and geophysical data.

Crustal and lithospheric thicknesses

The calculated crustal and lithospheric thicknesses resulting from the combined elevation and geoid data with thermal analysis are shown in Fig. 4, where the level of compensation is beneath the lithosphere-asthenosphere boundary (LAB).

Fig. 2 shows a compilation of proposed crustal thickness values, most of them using the receiver function's technique. The results are very variable according to different studies and seismic stations. The Mesopotamian foreland basin is characterized by crustal thicknesses between 38 and 45 km. The maximum Moho depths are situated along the Zagros mountain belt, beneath the Sanandaj–Sirjan Zone (Paul *et al.* 2010; Manaman *et al.* 2011). In general, these maximum values vary between 50 and 55 km, although Paul *et al.* (2010) propose values exceeding 65 km in SE Zagros. The crustal thickness in the Iranian block is ∼40–45 km increasing northwards to >50 km beneath the Alborz Mountains and ∼50 km in the Kopet Dag chain.

The resulting crustal thickness (Fig. 4a) varies from ∼40 to 44 km at the Mesopotamian foreland basin and Arabian platform to ∼55–62 km beneath the Zagros mountain belt. These values agree pretty well with those proposed from receiver function analysis by Gök *et al.* (2008) in the Arabian platform and Nasrabadi *et al.* (2008), Gritto *et al.* (2008) and Paul *et al.* (2010) in the Zagros. In the Iranian blocks the crustal thickness ranges between 40 and 44 km decreasing towards the SE where minimum values of < 36 km in the Lut basin and ∼38 km in the Jaz Murian basin are imaged. The Moho depth increases northwards to the Alborz Mountains with values between 48 and 56 km similar to those obtained by receiver functions (Doloei & Roberts 2003; Sodoudi *et al.* 2009; Radjaee *et al.* 2010), and towards the Kopet Dag Mountains with values between 45 and 54 km in agreement to Mangino & Priestley (1998) and Nowrouzi *et al.* (2007). The crustal thickness in the Southern Caspian region decreases to ∼36 km also in agreement with Mangino & Priestley (1998). These regional crustal thickness values are in general agreement with previous calculations from gravity (e.g. Snyder & Barazangi 1986) and seismic analyses

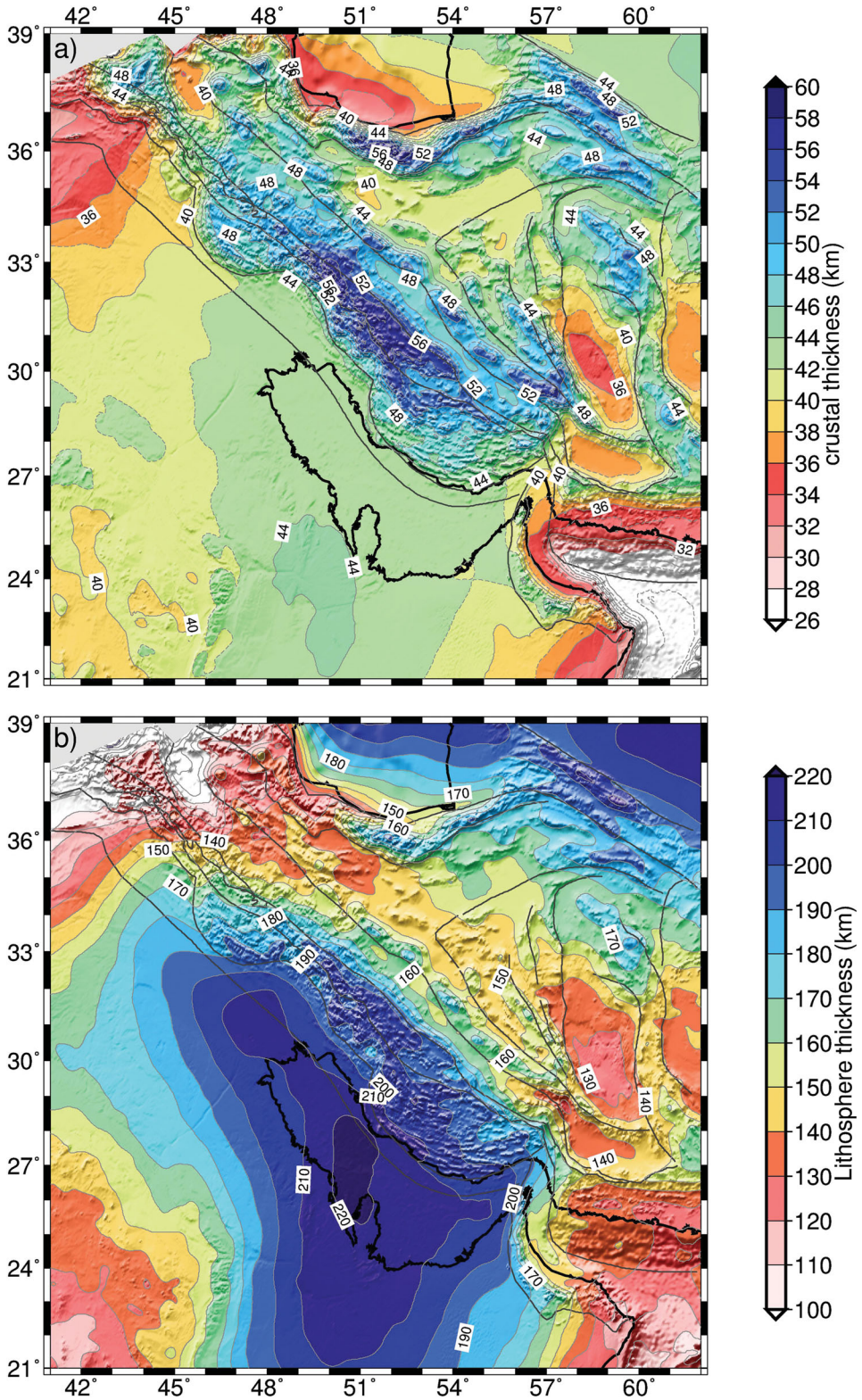

Figure 4. Resulting crustal (a) and lithospheric (b) thicknesses (contours every 2 and 10 km, respectively) obtained from combining elevation and geoid data. Shading indicates elevation.

(Manaman *et al.* 2011; and those values and references from Fig. 2). Although, Paul *et al.* (2010) in their southern profile (Zagros01, Fig. 2) obtained a deeper Moho underneath the Sanandaj–Sirjan zone, with crustal thicknesses up to 65 and 69 km. Our crustal model predicts lower values with the maximum thickness beneath the IZ. See also Fig. 2 for a compilation of available crustal thickness data in the study region

The Arabia–Eurasia collision zone is marked by a clear change on the lithosphere thickness with maximum and minimum values beneath the Mesopotamian foreland basin and the Iranian Plateau,

respectively (Fig. 4b). Most of this lithospheric thinning is produced across the Zagros mountain belt where the suture between the two plates, the MZF, is. The Arabian lithosphere is characterized by the maximum thickness in the study region with LAB depth values of more than 210 km, placed beneath the central Persian Gulf with a NW-SE and N-S trends. Along the Mesopotamian foreland basin the lithosphere thickness decreases from 200 to 100 km towards the Anatolian Plateau. The Iranian Plateau is characterized by LAB depths between 130 and 160 km with minimum values beneath the Lut and Jaz Murian basins of ∼125 and ∼135 km, respectively. This can be explained by the presence of a rheologically strong crust underneath these two basins, which causes accommodation of deformation on their edges (Jackson *et al.* 1990). The lithosphere-asthenosphere boundary dips again towards the N and NE in the Alborz and Kopet Dag mountains. This regional LAB geometry is in agreement with the shear wave velocity distribution obtained from Villaseñor *et al.* (2001) by inversion of S-wave arrival times and with the results from a seismic tomography experiment (Kaviani *et al.* 2007). According to Kaviani *et al.* (2007), the 0.5 km/s difference of Vs in the shallow mantle is likely due to a compositional change associated with higher temperatures beneath the Sanandaj–Sirjan Zone and the Urumieh-Dokhtar Arc than beneath the IZ. Kaviani *et al.* (2009) also suggested that the very coherent null splitting measurements that they found in the Zagros fold-and-thrust belt and the IZ, confirm that both domains are underlain by the same lithospheric mantle (of the Arabian platform). The velocity anomalies obtained by Alinaghi *et al.* (2007) show that the crust and upper mantle beneath the Iranian Plateau comprise a low velocity domain between the Arabian Plate and the Caspian Block. Sodoudi *et al.* (2009) interpreted the base of the lithosphere using S receiver functions at a depth of 90 km south of the Alborz Mountains, which is much shallower than our imaged 130 km.

Manaman & Shomali (2010) also found a sharp and steep subcrustal boundary coincident with the MZF, separating two different lithospheric mantle domains. The same authors attributed the high-velocity anomaly imaged beneath Central Iran at depths between 350 and 600 km as a fragment of subducted lithosphere. These observations as well as the sudden changes of shallow mantle velocities along a SW-NE profile crossing SE Zagros, with a sharp boundary under the Zagros suture zone, support the idea that subducted oceanic lithosphere has broken-off under the region of maximum crustal thickness. Lithospheric thinning beneath the Zagros mountain belt and the Iranian Plateau related to recent slab detachment or delamination has been also proposed by several authors (e.g. Bird 1978; Molinaro *et al.* 2005). Actually, lithospheric mantle thinning beneath orogens is not an uncommon feature as has also been evidenced beneath the Tibetan Plateau (Jiménez-Munt *et al.* 2008) and the Atlas Mountains (Teixell *et al.* 2005; Zeyen *et al.* 2005; Jiménez-Munt *et al.* 2011).

We performed a sensitivity test on the resulting crustal and lithosphere thicknesses by varying the removed harmonic spherical polynomials of the geoid height between degree and order 9th and 14th. Increasing the polynomial degree results in a less NW-SE tilting of geoid anomaly and consequently, in a thicker crust and lithosphere on the Arabian Plate (SW corner) and thinner on Iran. However, the variations on crustal and lithosphere thicknesses on the Zagros orogenic system are less than 1 km (<2 per cent) and 10 km (<7 per cent), respectively. Maximum crustal thickness variations are lower than 2 km (<8 per cent) in the Arabian shield whereas the lithosphere thickness varies between 15 and 17 km (∼10 per cent) in eastern Iran and between 12 and 20 km (10–22 per cent) in the Arabian shield.

An outstanding feature of our resulting lithospheric structure is the apparent large strain partitioning between the crust and the lithospheric mantle. This is evidenced by the differences of lateral variations in crust and mantle thickness and then by the regional deformation patterns. The crust show maximum thickness beneath the Zagros mountain belt and the Alborz and Kopet-Dag mountain belts coinciding with regions of high topography whereas minimum to normal values correspond to the Mesopotamian Basin and Arabian Platform. Interestingly, the lithospheric mantle shows an opposite deformation pattern with maximum thickness beneath the Mesopotamian Basin and Arabian Platform and minimum values towards the metamorphic domains of the Zagros mountain belt and the Iranian Plateau. These differences point to a major strain partitioning between the crust and the upper mantle (e.g. Bird 1978; Snyder & Barazangi 1986; Molinaro *et al.* 2005; Sobouti & Arkani-Hamed 1996). Limitations of the model are the use of potential field data, a simple vertical density distribution and the assumption of local isostasy and steady-state thermal regime. These limitations may result in an excessively smooth crustal and lithospheric mantle thickness geometry avoiding sharp lateral variations in the lithospheric structure.

Regional Bouguer gravity field

Once the crustal and lithospheric mantle structure is computed, the gravity effect of the model has been calculated to obtain the regional component of the Bouguer anomaly field. Calculations have been performed using the same crust and lithospheric mantle densities as in the process of combining the geoid and elevation data and thermal analysis. We have considered a density of 3200 kg m^{-3} for the asthenosphere and a reduction density of 2670 kg m^{-3} for water covered regions.

The computed regional gravity anomaly (Fig. 5) follows a trend similar to that of the long wavelength component of the observed Bouguer anomaly, and it mainly reflects the gravity anomalies related to deep-seated density variations. The elongated minimum of ∼−200 mGal beneath the Zagros results from the effect of the crustal root on the gravity signature. Towards the NE, in

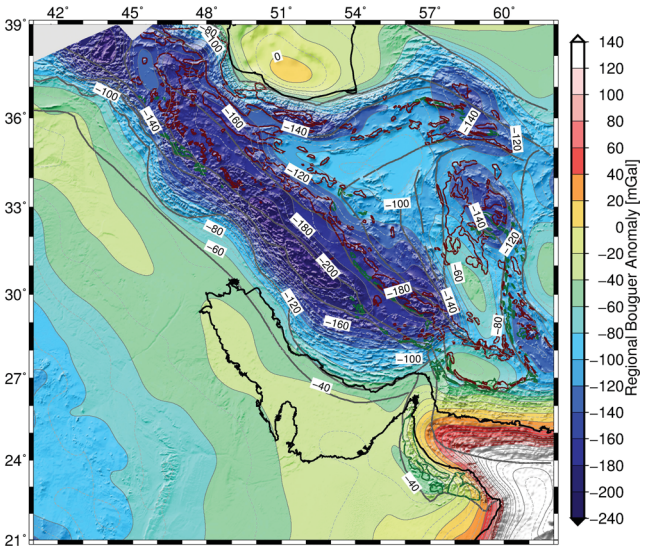

Figure 5. Regional Bouguer anomaly (contours every 10 mGal) calculated from the lithosphere structure obtained in Fig. 4. Red contours show the igneous complexes and green contours the ophiolite complexes. Shading indicates elevation.

Central Iran, the regional Bouguer anomaly increases to values of −100 mGal reflecting the combination of the competing effects related to crustal and lithospheric mantle thinning. The Mesopotamian foreland basin and Persian Gulf region is characterized by a relative maximum of ∼−40 mGal in a NW-SE direction related to the prominent lithospheric mantle thickening and 'normal' crust.

It is worth noting that using different methodologies in calculating the regional Bouguer anomaly such as filtering, crustal and lithospheric isostasy and combining elevation and geoid data, may result in similar field patterns but in conspicuous different amplitudes. In all these tested methods, the regional field is characterized by maximum values located in the Mesopotamian Foreland Basin and the Arabian Platform, minimum values along the Zagros and Alborz mountain belts, and intermediate values over Central Iran. However, using a Gaussian boxcar filter of 500 km wavelength results in the lower amplitude variations with a maximum value of ∼150 mGal. Considering local crustal isostasy (i.e. topography is fully compensated by crustal thickness variations) results in a maximum amplitude of ∼200 mGal which increases to >280 mGal when elevation is locally compensated by the crust and the lithospheric mantle under the additional assumption of pure shear deformation. The maximum amplitude corresponding to the presented method combining elevation and geoid data amounts ∼180 mGal and therefore is an intermediate value between filtering and local crustal isostasy. As it is explained in the next section, the election of the regional gravity field has an important influence on the interpretation of the residual Bouguer anomaly field.

Residual Bouguer gravity field

The regional Bouguer gravity field (Fig. 5) has been subtracted from the observed Bouguer anomaly (Fig. 3a) to calculate the residual Bouguer gravity field (Fig. 6). The latest reflects the distribution of lateral density variations within the crust and highlights concealed geological structures.

The obtained residual gravity anomaly map (Fig. 6) shows a good match between structural units and major changes of the residual gravity field. Local maximum are associated with outcrops of metamorphic basement and magmatic and ophiolitic rocks, whereas minimum values coincide with thick sediment accumulations in basins. The Mesopotamian–Persian Gulf foreland basin is characterized by an elongated minimum of −20 mGal in average.

At the large scale we can differentiate: (i) anomalies occurring in the undeformed Arabian Plate, (ii) a group of anomalies parallel to the tectonic units along the Zagros orogenic system, (iii) a strong positive anomaly that clearly delineates the Oman Mountain Belt, (iv) localized anomalies within the Iran blocks and (v) the anomalies related to the Alborz and Kopet Dag mountains.

The undeformed Arabian Plate

The undeformed Arabian Plate extends to the SW of the Cenozoic Zagros flexural basin (Mesopotamian–Persian Gulf foreland basin). The region is characterized by a relatively homogeneous and positive anomaly in its western region reaching local maxima of >20 mGal and a negative anomaly in the eastern region with values

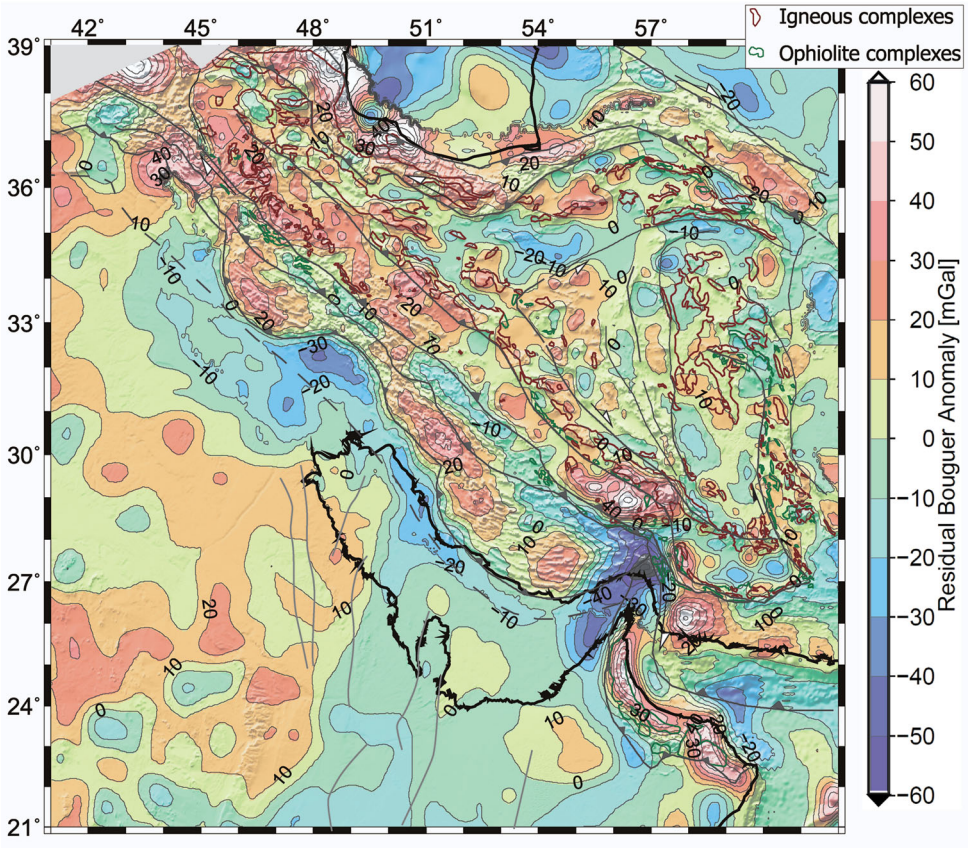

Figure 6. Residual Bouguer anomaly (contours every 10 mGal) resulting from subtracting the regional gravity (Fig. 5) to the measured (Fig. 3a). Red contours show the igneous complexes and green contours the ophiolite complexes.

down to −10 mGal. These two regions are separated by a well-defined N-S gravity boundary extending to the NW Persian Gulf.

The positive anomalies in the western part of the Arabian plate are related to the exposed Precambrian basement of the Arabian Shield that is gently dipping towards the NE. The negative anomalies in the eastern part coincide with the thick Phanerozoic succession in the Arabian Platform where the basement depth exceeds 8 km (Konert *et al.* 2001). The nearly N-S gravity boundary separating both regions coincides with the N-S trending set of faults affecting the basement onshore Arabia and beneath the Persian Gulf (Figs 1 and 6).

The Zagros orogenic system

In the Zagros orogenic system the residual Bouguer anomalies are organized, from SW to NE, in a series of positive and negative strips parallel to the main tectonic structures: (1) a minimum along the NW-SE trending Mesopotamian–Persian Gulf foreland basin, (2) a band with positive anomalies along the Simply Folded Belt, (3) a relatively continuous negative anomaly along the IZ, and (4) a wide and continuous positive residual anomaly band along both the Sanandaj–Sirjan Zone and the Urumieh-Dokhtar magmatic arc.

A fairly continuous NW-SE trending negative residual Bouguer anomaly (∼−20 mGal) is located along the front of the MFF corresponding to the position of the Mesopotamian–Persian Gulf foreland basin (Figs 1 and 6). Towards the SE, this NW-SE trending Persian Gulf negative residual Bouguer anomaly connects with a major NE-SW marked negative anomaly located along the northern front of the Oman Mountains. This anomaly is discussed in detail below.

The negative residual Bouguer anomaly along the Mesopotamian–Persian Gulf foreland basin completely matches the irregular geometry of this basin marked by the Kirkuk and the Dezful embayments and by the Pusht-e Kuh and Fars salients (Figs 1 and 6). To the NW of the Kirkuk embayment, however, the negative anomaly terminates against a strong positive anomaly coinciding with a basement high. The negative anomaly of the Dezful embayment fits with the basement depth map by Konert *et al.* (2001) showing maximum depths in this re-entrant and exceeding 11 km, from which the post-Oligocene sediments account for more than 6 km (Sepehr & Cosgrove 2004). The negative residual Bouguer anomaly of the Mesopotamian–Persian Gulf foreland basin is narrower along the front of the Fars arc due to the large-scale positive anomaly produced around the N-S trending Qatar Arch (Figs 1 and 6). Similar features can be observed in the NW side of the Persian Gulf where a roughly N-S trending positive anomaly impinges against the Mesopotamian–Persian Gulf negative anomaly (Fig. 6).

The Simply Folded Belt shows positive anomalies concentrated in the northern border of the Kirkuk embayment (>40 mGal), the Pusht-e Kuh arc (30–40 mGal), the SE Izeh Zone (>40 mGal) and the Fars arc (20–30 mGal). This general positive anomaly detected in the Simply Folded Belt is triggered by the elevated position of the basement-cover contact with respect to its position in the Mesopotamian foreland basin and Kirkuk and Dezful embayments (e.g. Falcon 1961; Emami *et al.* 2010). In the Fars arc the influence of the Qatar Arch produces a relative low in the average positive anomaly. The apparent contradiction between the existence of this gravity low and the Qatar basement high (e.g. Edgell 1996; Jahani *et al.* 2009) is probably related to the extent and distribution of the Hormuz evaporites over the region.

The IZ is defined by a narrow and elongated negative anomaly, with values down to −20 mGal. This elongated low is punctuated by relatively small regions showing positive anomalies that are related to shallower basement-cover contact position (Stern & Johnson 2010) (Fig. 6). The Imbricate Zone is characterized by the occurrence of ophiolites carried by low-angle thrust faults. The negative anomaly that extent along this tectonic unit can only be sustained if the outcropping ophiolites correspond to very thin slices overlying less dense material at shallow crustal depths. This implies the presence of either thicker cover sequences beneath the thrust sheets (see Vergés *et al.* 2011) or less dense intrusive magmatic bodies whose existence is more difficult to confirm. The negative Bouguer anomaly extends along the NE border of the Fars arc (the Imbricate Zone in very narrow along the SE Zagros). This anomaly merges with the roughly N-S trending large anomaly constricted between the SE Fars arc and the northern Oman Mountains (Fig. 6). In this context, the connection of the N-S Strait of Hormuz negative anomaly with the negative anomaly along the NE border of the Fars arc (and Imbricate Zone) would possibly strengthen the interpretation of a thicker cover sequence beneath the thrust system of the Imbricate Zone tectonic unit.

The Sanandaj–Sirjan Zone shows a wide band of positive anomalies, with the maximum values to the NW and SE reaching >50 mGal in close coincidence with ophiolitic belts. The Urumieh-Dokhtar Arc also shows a broad positive anomaly that must be related, as in the case of the Sanandaj–Sirjan Zone, to the large outcrop of metamorphic and non-metamorphic Mesozoic and Paleozoic rocks.

The Oman Mountains and the Makran accretionary wedge

To the SE of the Zagros orogenic system, a very strong-coupled positive-negative anomaly (Fig. 6) delineates the Oman Mountain belt and its foreland basin. The minimum residual Bouguer anomaly reaches values between −40 and −60 mGal whereas the maximum values are over 50 mGal along the northern segment of the Oman Mountains.

The strong negative anomaly detected along the northern boundary of the Oman Mountains is related to the northern continuation of the Oman foreland basin, presently below the Hormuz Straits. This area shows a complex structure characterized by the junction of the Zagros front along the southern Fars arc segment, the Oman Mountains front and the Minab Fault Zone. The Oman Mountains front was uplifted during the Tertiary and then covered again by middle-late Miocene sediments (e.g. Boote *et al.* 1990; Ravaut *et al.* 1997; Jahani *et al.* 2009).

The negative residual anomaly along the Oman foreland basin shows an arcuate geometry, parallel to the Oman Mountains trend, and extends beyond the structural line formed by the Zagros and Minab thrust fault zone (Fig. 6). The Oman foreland basin is characterized by 6–8 km thick Late Cretaceous to Pliocene syntectonic sedimentary succession. The strong positive anomaly observed along the Oman Mountains is related to the occurrence of the ∼6-km thick Ophiolite complex and its metamorphic sole emplaced during the obduction stage.

NE of the Oman Gulf, the Makran accretionary wedge is divided into a negative domain (<−30 mGal) offshore, and a positive domain (>60 mGal) onshore. Although only Tertiary flysch rocks are exposed at surface in this area, the large positive anomaly suggests the occurrence of dense imbricated rocks at depth, as already proposed by Shahabpour (2010). North of the Makran prism, the Jazz Murian basin is characterised by a new area of negative

anomalies (∼−20 mGal), probably related to a relatively thick sedimentary succession.

The Iranian block

The Iranian block define a complex area formed by several minor blocks separated by compressive belts and minor flexural basins individualised during the long Eurasia-Arabia convergence period (Fig. 1). This complexity is also evident in the residual Bouguer anomaly, which does not display regional trends as in other areas but is characterised by an irregular distribution with values between −30 and 30 mGal (Fig. 6). Comparing with surface geology, we can correlate these residual anomalies to tectonic elements.

The main negative anomaly is located in the NW Iran block, between the Central Iranian blocks, the Urumieh-Dokhtar arc and the Alborz Mountains, corresponding to the Qom basin, the Great Kabir basin and the Alborz foreland basin (Figs 1 and 6). To the east, a minimum of about −30 mGal corresponds to a thickness of about 5 km of alternate evaporites and limestones deposited in the Great Kavir (Jackson *et al.* 1990). To the west, a minimum of about −20 mGal corresponds to a maximum thickness of Tertiary sediments of about 12 km (Morley *et al.* 2009). Around these basins, positive anomalies are associated with basement highs and igneous complexes.

In the SW part, a wide negative anomaly (−10 mGal) can be observed in the Lut basin, a long living basin with a thick sedimentary succession, bounded in the north by large igneous complexes associated to local maxima (>10 mGal) and in the west by the Sistan Suture, an ophiolite belt also associated to local maxima (>20 mGal). The northern border of the Central Iranian blocks is also defined by a narrow negative anomaly (−20 mGal).

The Alborz and the Kopet Dag mountain belts

The northern border of the Iranian block is defined by the Alborz and Kopet Dag mountain belts, associated with positive residual anomalies of 40–60 mGal and <30 mGal, respectively (Fig. 6). The positive anomaly in the Alborz Mountains is in agreement with relatively simple anticlinorium geometry with a shallower basement along its axis. The high values of the residual anomaly in the western part can be correlated with the distribution of the igneous complexes (Figs 1 and 6). The Kopet Dag Mountain Belt corresponds to a continuous positive anomaly band bounded by minimum anomalies of <−20 mGal and <−30 mGal in the SW and NE, respectively, and associated with sedimentary basins.

We also studied the effect of changing the crustal density gradient of the model on the residual Bouguer anomaly and the lithosphere structure. The results show that the pattern of the residual Bouguer anomaly is independent of the crustal density gradient and only the amplitudes change slightly. Preserving the average crustal density but considering a higher density gradient, between 2670 kg m^{-3} at surface and 3010 kg m^{-3} at Moho depth, the differences of the residual Bouguer anomaly are less than 5 per cent. The newly calculated crustal and lithosphere thicknesses show variations relative to the proposed model of less than 1 and 2 per cent, respectively.

Comparing different residual Bouguer anomaly fields

As mentioned before the measured Bouguer anomaly can be separated into a regional and a residual or local component, and this separation is very sensitive to the used methodology. In a previous section we discussed the differences between the regional Bouguer anomaly fields obtained by filtering, crustal isostasy (Airy model), lithosphere isostasy and combining elevation and geoid. In this section we illustrate the significance of considering different residual Bouguer anomalies in terms of shallow geology, main tectonic units, and related lithospheric structures along a profile crossing the entire Zagros mountain belt and its foreland basin (Fig. 7; location of profile in Fig. 2).

1. Using a Gaussian boxcar filter with a wavelength of 500 km (Fig. 7b), the Mesopotamian–Persian Gulf foreland basin practically has no associated residual anomaly with values between −10 and 10 mGal. In contrast, part of the Folded Belt and the IZ are characterized by negative values with the minimum residual anomaly (∼−40 mGal) beneath the contact between the IZ and the Sanandaj–Sirjan Zone. Surprisingly, the amplitude of this negative anomaly is noticeably higher than that of the Mesopotamian–Persian Gulf foreland basin. Therefore, the residual anomalies obtained by filtering appear to be poorly correlated with surface geology.
2. Assuming a crustal isostatic model the results are more similar to those obtained from elevation and geoid data (with differences up to 30 mGal in the Mesopotamian–Persian Gulf foreland basin). The minimum values (∼−55 mGal) are located in the foreland basin whereas the maximum values are located in the Central Iranian Blocks (∼40 mGal) (see also Snyder & Barazangi 1986). Curiously, the residual anomaly derived by crustal isostasy appears to be tilted with respect to that obtained by elevation and geoid being the hinge point at the Sanandaj–Sirjan Zone. Implicit to this method is that the base of the lithosphere is flat (Fig. 7c), which is difficult to sustain in a tectonic context characterized by continental collision and subduction (e.g. Agard *et al.* 2011). Moreover, the amplitude of the geoid height obtained from this lithosphere structure (∼12 m) is much lower than measured (∼24 m) (Fig. 7d).
3. Assuming a lithosphere isostasy model results in a residual gravity anomaly characterized by large variations due to the large lateral changes in crustal and lithosphere thicknesses (Fig. 7). The Mesopotamian foreland shows a minimum exceeding −90 mGal, whereas the Zagros mountain belt and the Iranian Plateau are represented by positive anomalies, with maximum values over 85 mGal in the Sanandaj–Sirjan Zone. This results in total amplitude exceeding 180 mGal, which is an extraordinarily high value to be related to shallow structures. Certainly, this model results in crustal thickness values beneath the Zagros orogenic system that are in close agreement with those propose by Paul *et al.* (2006, 2010) from receiver function analyses. However, the compensation of the obtained crustal structure requires a thick lithosphere beneath the Zagros and a relatively thin lithosphere beneath the Mesopotamian–Persian Gulf foreland basin (Fig. 7c). This lithosphere structure is in clear disagreement with the seismic velocity anomalies resulting from tomographic models, which predict low velocities and then hot lithosphere beneath the NE Zagros and Iranian Plateau (Manaman & Shomali 2010). Likewise, the calculated geoid height shows an inverse trend than observed with positive values in the foreland basin region and negative values in the orogenic belt (Fig. 7d).

CONCLUDING REMARKS

The method used, based on the fitting of elevation and geoid height data combined with thermal analysis, allows for a rapid

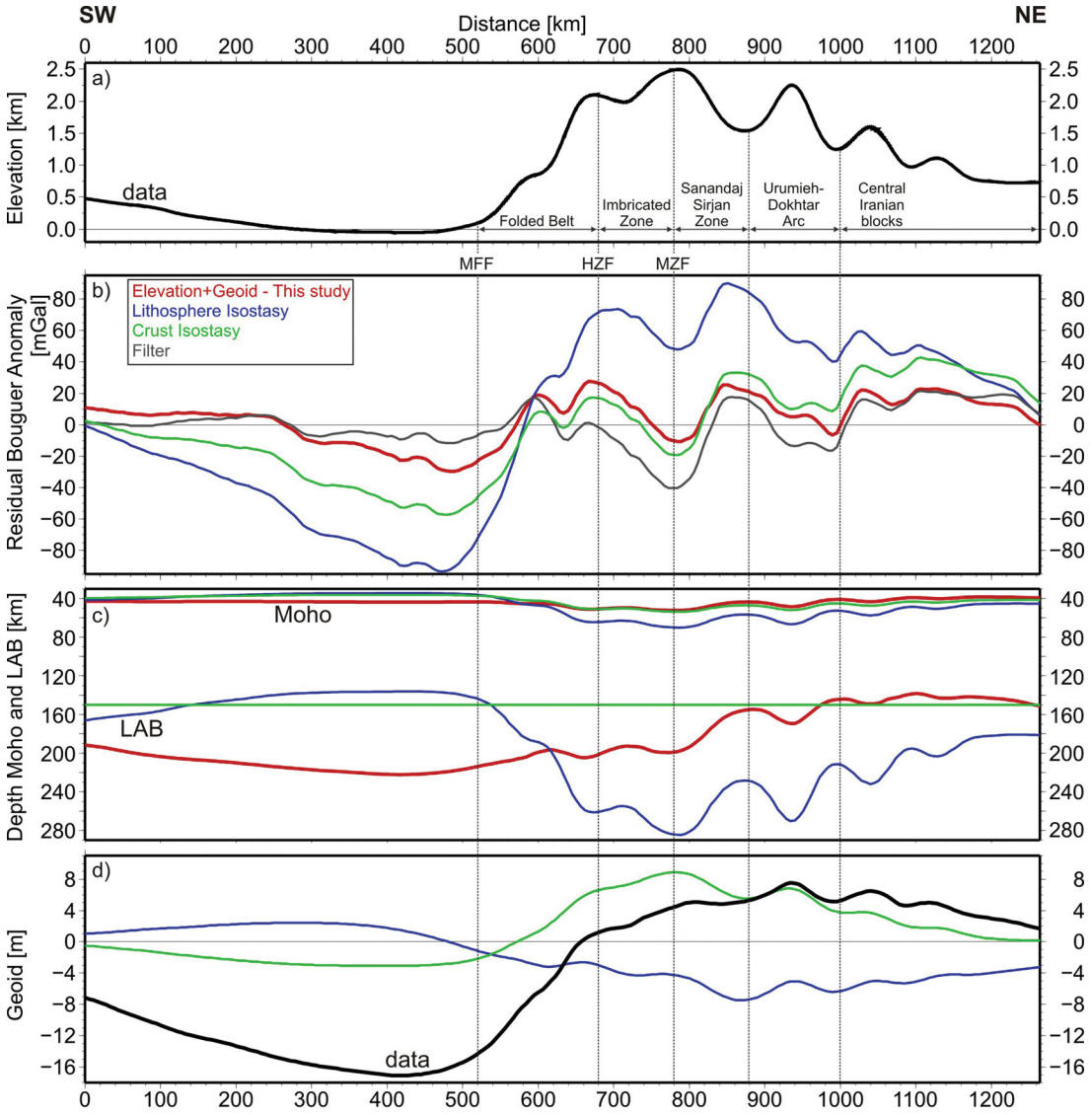

Figure 7. Comparison between different methods of calculating the residual gravity anomaly, along a profile located on Fig. 2. (a) Topography data. (b) Residual Bouguer anomalies. (c) Moho and LAB depths. (d) Geoid data and calculated from the different lithospheres structures. Each colour line represents the result from: red for combining geoid and elevation; grey for Gaussian filter at 500 km; green for crustal isostasy (Airy); blue for lithosphere isostasy; and thick black line for data.

calculation of the crustal and lithospheric thickness over large regions under the assumption of local isostasy and thermal steady state. The new methodology used in separating the residual Bouguer anomaly from the total gravity field results in noticeable differences with respect to methods based on filtering, and crustal and lithosphere isostasy, and shows a better correlation with geological structures.

The crustal and lithospheric mantle structure obtained for the Arabia–Eurasia collision zone coincides fairly well with previous analyses based on seismic experiments, regional tomography and integrated modelling. Maximum crustal thickness values of ∼60 km are located along the IZ between Fars and Lurestan arcs decreasing to ∼42 km towards the Mesopotamian foreland basin and the Persian Gulf and towards the Central Iranian Block. The minimum values are found in the Lut (<36 km) and Jaz Murian (<38 km) basins. The Alborz and Kopet Dag mountains show crustal thicknesses around 50 km.

The most outstanding result is the distinct deformation patterns between the crust and the lithospheric mantle beneath the Zagros mountain belt indicating a strong strain partitioning in the region. The lithosphere thickens beneath the down-flexed Arabian Plate from the Kirkuk Embayment to the Oman Arc with LAB-depth values between 150 and 210 km. Maximum values exceeding 220 km are found in the Persian Gulf and the Qatar Arch following the N-S fault system separating the Arabian Shield from the Rub' al-Khali basin. Minimum lithospheric thickness values (<140 km) are located to the NW of the Zagros (Iranian Plateau) and to the SE (Lut and Jaz Murian basins and Makran and Oman Gulf). Interestingly, the Zagros mountain belt is affected by a progressive lithospheric thinning from the Mesopotamian foreland basin (∼210 km) to the

Central Iranian Block (<160 km). The LAB deepens again to the NE towards the Alborz and Kopet Dag mountains and the Eurasian Plate.

The analysis of the residual anomalies across the Zagros orogenic system indicates that: (i) the negative residual in the Mesopotamian foreland basin and the Persian Gulf is compatible with a strong down-flexure of the basement from early Tertiary times; (ii) the positive residual in the Simply Folded Belt indicates a shallower basement with respect to the foreland basin and the IZ; (iii) the negative residual in the IZ suggests that the outcropping ophiolites must correspond to thin slices overlying a thick sedimentary sequence or low density magmatic intrusive bodies; and (iv) the positive residual anomaly corresponding with the Sanandaj–Sirjan and Urumieh-Doktar zones is related to metamorphic and igneous/ophiolite complexes.

ACKNOWLEDGMENTS

This research has been partly funded by Projects ATIZA (CGL2009-09662-BTE) and TECLA (CGL2011–26670) and Consolider-Ingenio 2010 Topo-Iberia (CSD2006-00041). We thank DARIUS Programme for their additional support. Constructive reviews from Jörg Ebbing and an anonymous reviewer, as well as the advice of the Editor Bert Vermeersen, helped us to improve the final version.

REFERENCES

Agard, P. *et al*., 2011. Zagros orogeny: a subduction-dominated process, *Geol. Mag.,* **148,** 692–725, doi:10.1017/S001675681100046X.

Alavi, M., 1994. Tectonics of the Zagros orogenic belt of Iran: new data and interpretations, *Tectonophysics,* **229,** 211–238.

Al-Damegh, K., Sandvol, E., Al-Lazki, A. & Barazangi, M., 2004. Regional seismic wave propagation (Lg and Sn) and Pn attenuation in the Arabian Plate and surrounding regions, *Geophys. J. Int.,* **157,** 775–795.

Alinaghi, A., Koulakov, I., Thybo, H., 2007. Seismic tomographic imaging of P- and S-waves velocity perturbations in the upper mantle beneath Iran, *Geophys. J. Int.,* **169,** 1089–1102, doi:10.1111/j.1365-246X.2007.03317.x.

Allemann, F. & Peters, T., 1972. The ophiolite-radiolarite belt of the North Oman mountains, *Eclogae Geol. Helv.,* **65,** 657–698.

Amante, C. & Eakins, B.W., 2009. ETOPO1 1 Arc-Minute Global Relief Model: Procedures, Data Sources and Analysis. NOAA Technical Memorandum NESDIS NGDC-24, 19pp. Available at: http://www.ngdc.noaa.gov (last accessed 2009 November).

Ardalan, A.A., Zamzam, D. & Karimi, R., 2011. An alternative method for density variation modeling of the crust based on 3-D gravity inversion, *J. appl. Geophys.,* **75,** 355–362, doi:10.1016/j.jappgeo.2011.06.033.

Baharifar, A., Moinevaziri, H., Bellon, H. & Pique, A., 2004. The crystalline complexes of Hamadan (Sanandaj–Sirjan zone, western Iran): metasedimentary Mesozoic sequences affected by Late Cretaceous tectono-metamorphic and plutonic events, *Comptes Rendues Geosci.,* **336**(16), 1446–1452.

Bahroudi, A. & Koyi, H.A., 2003. Effect of spatial distribution of Hormuz salt in deformation style in the Zagros fold-and-thrust belt: an analogue modelling approach, *J. geol. Soc. Lond.,* **160,** 719–733.

Ballato, P., Uba, C.E., Landgraf, A., Strecker, M.R., Sudo, M., Stockli, D.F., Friedrich, A. & Tabatabaei, S.H., 2011. Arabia–Eurasia continental collision: insights from late tertiary foreland-basin evolution in the Alborz Mountains, Northern Iran, *Bull. geol. Soc. Am.,* **123**(1–2), 106–131.

Berberian, M., 1995. Master blind thrust faults hidden under the Zagros folds: active basement tectonics and surface morphotectonics, *Tectonophysics,* **241,** 193–224.

Berberian, F. & Berberian, M., 1981. Tectono-plutonic episodes in Iran, in *Zagros, Hindu Kush, Himalaya: Geodynamic Evolution,* Geodyn. Ser. Vol. 3, pp. 5–32, eds Gupta, H.K. & Delany, F.M., American Geophysical Union, Washington, DC.

Berberian, F., Muir, I.D., Pankhurst, R.J. & Berberian, M., 1982. Late cretaceous and early Miocene Andean-type plutonic activity in northern Makran and Central Iran, *J. geol. Soc. London,* **139,** 605–614.

Bernard, D., Caillat, C., Dehlavi, P., Martel-Jentin, B. & Vivier, G., 1979. *Premières données géochronométriques sur les roches intrusives de la région de Saveh (Iran) 7ème R.A.S.T.,* Société Géologique de France, Lyon, 48pp.

Bina, M.M., Bucur, I., Prevot, M., Meyerfeld, Y., Daly, L., Cantagrel, J.M. & Mergoil, J., 1986. Palaeomagnetism, petrology and geochronology of tertiary magmatic and sedimentary units from Iran, *Tectonophysics,* **121**(2–4), 303–329.

Bird, P., 1978. Finite-element modelling of the lithosphere deformation: the Zagros collision orogeny, *Tectonophysics,* **50,** 307–336.

Boote, D.R.D., Mou, D. & Waite, R.I., 1990. Structural evolution of the Suneinah Foreland, Central Oman Mountains, *Geol. Soc., Lond., Special Publications,* **49,** 397–418, doi:10.1144/GSL.SP.1992.049.01.25.

Bowin, C., 2000. Mass anomalies and the structure of the Earth, *Phys. Chem. Earth,* **25**(4), 343–353.

Braud, J., 1970. Les formations du Zagros dans la région de Kermanshah (Iran) et leur rapport structuraux. C. R, *Acad. Sci. Paris,* **271,** 1241–1244.

Braud, J., 1987. *La suture du Zagros au niveau de Kermanshah (Kurdistan Iranien): reconstitution paléogéographique, évolution géodynamique, magmatique et structurale,* Université Paris-Sud, Paris, 450pp.

Burg, J.-P., Bernoulli, D., Smit, J., Dolati, A. & Bahroudi, A., 2008. A giant catastrophic mud-and-debris flow in the Miocene Makran, *Terra Nova,* **20**(3), 188–193.

Casciello, E., Vergés, J., Saura, E., Casini, G., Fernández, N., Blanc, E., Homke, S. & Hunt, D., 2009. Fold patterns and multilayer rheology of the Lurestan Province, Zagros Simply Folded Belt (Iran), *J. Geol. Soc. Lond.,* **166,** 947–959, doi:10.1144/0016-76492008-138.

Dehghani, G. & Makris, J., 1984. The gravity field and crustal structure of Iran, *N. Jahrb. Geol. Palaont. Abh. Stuttgart,* **168,** 215–229.

Doloei, J. & Roberts, R., 2003. Crust and uppermost mantle structure of Tehran region from analysis of teleseismic P-waveform receiver functions, *Tectonophysics,* **364,** 115–133.

Edgell, H.S., 1996. Salt tectonism in the Persian Gulf Basin, *Geol. Soc., Lond., Special Publications,* **100,** 129–151, doi:10.1144/GSL.SP.1996.100.01.10.

Ellouz-Zimmermann, N. *et al*., 2007. Offshore frontal part of the Makran accretionary prism: the Chamak survey (Pakistan), in *Thrust Belts and Foreland Basins from Fold Kinematics to Hydrocarbon Systems,* Frontiers in Earth Sciences, pp. 351–368, Chapter 18, eds Lacombe, O., Lavé, J., Roure, F., Verges, J., Springer, Berlin.

Emami, H., Vergés, J., Nalpas, T., Gillespie, P., Sharp, I., Karpuz, R., Blanc, E.P. & Goodarzi, M.G.H., 2010. Structure of the mountain front flexure along the Anaran anticline in the Pusht-e Kuh Arc (NW Zagros, Iran): insights from sand box models, *Geol. Soc., Lond., Special Publications,* **330,** 155–178, doi:10.1144/SP330.9.

Falcon, N.L., 1961. Major earth-flexuring in the Zagros Mountains of south-west Iran, *Q. J. geol. Soc. Lond.,* **117**(4), 367–376.

Falcon, N.L., 1967. The geology of the north-east margin of the Arabian basement shield, *Advancement Sci.,* **24,** 1–12.

Fullea, J., Fernàndez, M., Zeyen, H. & Vergés, J., 2007. A rapid method to map the crustal and lithospheric thickness using elevation, geoid anomaly and thermal analysis. Application to the Gibraltar Arc System, Atlas Mountains and adjacent zones, *Tectonophysics,* **430,** 97–117.

Fullea, J., Fernández, M. & Zeyen, H., 2008. FA2BOUG—A FORTRAN 90 code to compute Bouguer gravity anomalies from gridded free air anomalies: Application to the Atlantic-Mediterranean transition zone, *Comput. Geosci.,* **34,** 1665–1681, doi:10.1016/j.cageo.2008.02.018.

Glennie, K.W., Hughes Clarke, M.W., Boeuf, M.G.A., Pilaar, W.F.H. & Reinhardt, B.M., 1990. Inter-relationship of Makran-Oman Mountains

belts of convergence, *Geol. Soc., Lond., Special Publications,* **49,** 773–786, doi:10.1144/GSL.SP.1992.049.01.47.

Glumov, I.F., Malovitskiy, Y.P., Novikov, A.A. & Senin, B.V., 2004. *Regional Geology and Oil and Gas Content of Caspian Sea,* Nedra, Moscow (in Russian).

Gök, R., Mahdi, H., Al-Shukri, H. & Rodgers, A.J., 2008. Crustal structure of Iraq from receiver functions and surface wave dispersion: implications for understanding the deformation history of the Arabian–Eurasian collision, *Geophys. J. Int.,* **172,** 1179–1187, doi:10.1111/j.1365-246X.2007.03670.x.

Golonka, J., 2004. Plate tectonic evolution of the southern margin of Eurasia in the Mesozoic and Cenozoic, *Tectonophysics,* **381,** 235–273.

Gritto *et al*., 2008. Crustal structure of North Iraq from receiver function analyses, 2008 monitoring research review: ground-based nuclear explosion monitoring technologies. Contract No. FA8718–07-C-0008.

Hatzfeld, D. & Molnar, P., 2010. Comparisons of the kinematics and deep structures of the Zagros and Himalaya and of the Iranian and Tibetan Plateaus and geodynamic implications, *Rev. Geophys.,* **48,** RG2005, doi:10.1029/2009RG000304.

Jackson, Martin, P.A., Cornelius, R.R., Craig, C.H., Gansser, A., Stocklin, J. & Talbot, C.J., 1990. Salt diapirs of the Great Kavir, Central Iran, *Geol. Soc. Am. Memoir,* **177,** 139pp.

Jahani, S., Callot, J.P., Letouzey, J. & De Lamotte, D.F., 2009. The eastern termination of the Zagros Fold-and-Thrust Belt, Iran: structures, evolution, and relationships between salt plugs, folding, and faulting, *Tectonics,* **28**(6), TC6004, doi:10.1029/2008TC002418.

Jiménez-Munt, I., Fernàndez, M., Vergés, J. & Platt, J.P., 2008. Lithosphere structure underneath the Tibetan Plateau inferred from elevation, gravity and geoid anomalies, *Earth. Planet. Sci. Lett.,* **267,** 276–289, doi:10.1016/j.epsl.2007.11.045.

Jiménez-Munt, I., Fernàndez, M., Vergés, J., Garcia-Castellanos, D., Fullea, J., Pérez-Gussinyé, M. & Afonso, J.C., 2011. Decoupled accomodation of Africa-Eurasia convergence in the NW-Moroccan margin, *J. geophys. Res.,* **116,** B08403, doi:10.1029/2010JB008105.

Kaviani, A., Paul, A., Bourova, E., Hatzfeld, D., Pedersen, H. & Mokhtari, M., 2007. A strong seismic velocity contrast in the shallow mantle across the Zagros collision zone (Iran), *Geophys. J. Int.,* **171,** 399–410, doi:10.1111/j.1365-246X.2007.03535.x.

Kaviani, A., Hatzfeld, D., Paul, A., Tatar, M. & Priestley, K., 2009. Shear-wave splitting, lithospheric anisotropy, and mantle deformation beneath the Arabia–Eurasia collision zone in Iran, *Earth. Planet. Sci. Lett.,* **286,** 371–378, doi:10.1016/j.epsl.2009.07.003.

Kent, P.E., 1979. The emergent Hormuz salt plugs of Southern Iran, *J. Petrol. Geol.,* **2(2)**, 117–144.

Kiamehr, R., 2006. The impact of lateral density variation model in the determination of precise gravimetric geoid in mountainous areas: a case study of Iran, *Geophys. J. Int.,* **167,** 521–527, doi:10.1111/j.1365-246X.2006.03143.x.

Konert, G., Afifi, A.M., Al-Harjri, S.A. & Droste, H.J., 2001. Paleozoic stratigraphic and hydrocarbon habitat of the Arabian Plate, *GeoArabia,* **6,** 407–442.

Leterrier, J., 1985. Mineralogical, geochemical and isotopic evolution of two Miocene mafic intrusions from the Zagros (Iran), *Lithos,* **18,** 311–329.

Mangino, M. & Priestley, K., 1998. The crustal structure of the southern Caspian region, *Geophys. J. Int.,* **133,** 630–648.

Manaman, N.S. & Shomali, H., 2010. Upper mantle S-velocity structure and Moho depth variations across Zagros belt, Arabian–Eurasian plate boundary, *Phys. Earth planet. Inter.,* **180,** 92–103, doi:10.1016/j.pepi.2010.01.011.

Manaman, N.S., Shomali, H. & Koyi, H., 2011. New constraints on upper-mantle S-velocity structure and crustal thickness of the Iranian plateau using partitioned waveform inversion, *Geophys. J. Int.,* **184,** 247–267, doi:10.1111/j.1365-246X.2010.04822.x.

Martel-Jentin, B., Caillat, C., Dehlavi, P. & Vivier, G., 1979. Géochimie du volcanisme et du plutonisme paléogènes de la région de Saveh (Iran). Origine des tendances alcalines et calco-alcalines du Paléogène de la zone de l'Iran Central, 7ème R.A.S.T. Société Géologique de France, Lyon, 314pp.

Masoudi, F., 1997. Contact metamorphism and pegmatite development in the SW of Arak, Iran, *PhD thesis*, University of Leeds, 231pp.

McCall, G.J.H. & Kidd, R.G.W., 1982. The Makran, Southeastern Iran: the anatomy of a convergent plate margin active from Cretaceous to Present, *Geol. Soc., Lond., Special Publications,* **10**(1), 387–397, doi:10.1144/GSL.SP.1982.010.01.26.

Molinaro, M., Zeyen, H. & Laurencin, X., 2005. Lithospheric structure beneath the south-eastern Zagros Mountains, Iran: recent slab break-off?, *Terra Nova,* **17,** 1–6, doi:10.1111/j.1365-3121.2004.00575.x.

Morley, C.K. *et al*., 2009. Structural development of a major late Cenozoic basin and transpressional belt in central Iran: the Central Basin in the Qom-Saveh area, *Geosphere,* **5**(4), 325–362.

Motavalli-Anbaran, S.-H., Zeyen, H., Brunet, M.-F. & Ardestani, V.E., 2011. Crustal and lithospheric structure of the Alborz Mountains, Iran, and surrounding areas from integrated geophysical modeling, *Tectonics,* **30**(5), TC5012, doi:10.1029/2011TC002934.

Nasrabadi, A., Tatar, M., Priestley, K. & Sepahvand, M.R., 2008. Continental lithosphere structure be neath the Iranian Plateau, from analysis of receiver functions and surfaces waves dispersion, *The 14th World Conference on Earthquake Engineering, 2008 October 12–17*, Beijing, China.

Nemati, M. & Yassaghi, A., 2010. Structural characteristics of the transitional zone from internal to external parts of the Zagros orogen, Iran, *J. Asian Earth Sci.,* **39**(3), 161–172.

Nowrouzi, G., Priestley, K., Ghafory-Ashtiany, M., Doloei, J. & Rham, D., 2007. Crustal velocity structure in the Kopet-Dagh, from analysis of P-waveform receiver functions, *J. Seismo. Earthq. Eng.,* **8,** 187–194.

Paul, A., Kaviani, A., Hatzfeld, D., Vergne, J. & Mokhtari, M., 2006. Seismological evidence for crustal-scale thrusting in the Zagros mountain belt (Iran), *Geophys. J. Int.,* **166,** 227–237.

Paul, A., Hatzfeld, D., Kaviani, A., Tatar, M. & Péquegnat, C., 2010. Seismic imaging of the lithospheric structure of the Zagros mountain belt (Iran), *Geol. Soc., Lond., Special Publications,* **330,** 5–18, doi:10.1144/SP330.2.

Pavlis, N.K., Holmes, S.A., Kenyon, S.C. & Factor, J.K., 2008. An Earth Gravitational Model to Degree 2160: EGM2008, *2008 General Assembly of the European Geosciences Union*, Vienna, Austria, 2008 April 13–18.

Radjaee, A., Rham, D., Mokhtari, M., Tatar, M., Priestley, K. & Hatzfeld, D., 2010. Variation of Moho depth in the central part of the Alborz Mountains, northern Iran, *Geophys. J. Int.,* **181,** 173–184, doi:10.1111/j.1365-246X.2010.04518.x.

Ravaut, P., Bayer, R., Hassani, R., Rousset, D. & Al Yahya'ey, A., 1997. Structure and evolution of the northern Oman margin: gravity and seismic constraints over the Zagros-Makran-Oman collision zone, *Tectonophysics,* **279**(1–4), 253–280.

Sandwell, D.T. & Smith, W.H.F., 1997. Marine gravity anomalies from GEOSAT and ERS-1 satellite altimetry, *J. Geophys. Res.,* **102,** 10039–10054.

Saura, E. *et al*., 2011. Basin architecture and growth folding of the NW Zagros early foreland basin during the Late Cretaceous and early Tertiary, *J. Geol. Soc.,* **168**(1), 235–250.

Sepehr, M. & Cosgrove, J.W., 2004. Structural framework of the Zagros Fold-Thrust Belt, Iran, *Mar. Petrol. Geol.,* **21**(7), 829–843.

Shahabpour, J., 2010. Tectonic implications of the geochemical data from the Makran igneous rocks in Iran, *Island Arc,* **19**(4), 676–689.

Snyder, D.B. & Barazangi, M., 1986. Deep crustal structure and flexure of the Arabian Plate beneath the Zagros collisional mountain belt as inferred from gravity observations, *Tectonics,* **5**(3), 361–373.

Sobouti, F. & Arkani-Hamed, J., 1996. Numerical modelling of the deformation of the Iranian plateau, *Geophys. J. Int.,* **126,** 805–818.

Sodoudi, F., Yuan, X., Kind, R., Heit, B. & Sadidkhouy, A., 2009. Evidence for a missing crustal root and a thin lithosphere beneath the Central Alborz by receiver function studies, *Geophys. J. Int.,* **177,** 733–742, doi:10.1111/j.1365-246X.2009.04115.x.

Stern, R.J. & Johnson, P., 2010. Continental lithosphere of the Arabian Plate: a geologic, petrologic, and geophysical synthesis, *Earth-Sci. Rev.,* **101,** 29–67.

Stocklin, J., 1968. Salt deposits of the Middle East, *Geol. Soc. Am. Special Paper,* **88,** 158–181.

Stoneley, R., 1975. On the origin of ophiolite complexes in the southern Tethys region, *Tectonophysics,* **25**(3–4), 303–322.

Teixell, A., Ayarza, P., Zeyen, H., Fernandez, M. & Arboleya, M.L., 2005. Effects of mantle upwelling in a compressional setting: the Atlas Mountains of Morocco, *Terra Nova,* **17,** 456–461.

Valizadeh, M.V. & Cantagrel, J.M., 1975. K-Ar and Rb-Sr radiometric data on micas from Mt-Alvand granitic complex near Hamadan (Western Iran), *Comptes Rendus de l'Academie des Sci.,* **281**(15), 1083–1086.

Vergés, J., Saura, E., Casciello, E., Fernàndez, M., Villaseñor, A., Jiménez-Munt, I. & Garcia-Castellanos, D., 2011. Crustal-scale cross-section across the NW Zagros Belt: implications for the Arabian Margin reconstructions, *Geol. Mag.,* **148,** 739–761, doi:10.1017/S0016756811000331.

Vilà, M., Fernàndez, M. & Jiménez-Munt, I., 2010. Radiogenic heat production variability of some common lithological groups and its significance to lithospheric thermal modeling, *Tectonophysics,* **490,** 152–164, doi:10.1016/j.tecto.2010.05.003.

Villaseñor, A., Ritzwoller, M.H., Levshin, A.L., Barmin, M.P., Engdahl, E.R., Spakman, W. & Trampert, J., 2001. Shear velocity structure of central Eurasia from inversion of surface wave velocities, *Phys. Earth planet. Inter.,* **123,** 169–184.

Zeyen, H., Ayarza, P., Fernàndez, M. & Rimi, A., 2005. Lithospheric structure under the western African–European plate boundary: a transect across the Atlas Mountains and the Gulf of Cadiz, *Tectonics,* **24,** TC2001, doi:10.1029/2004TC001639.

SUPPORTING INFORMATION

Additional Supporting Information may be found in the online version of this article:

Figure S1. Regional Bouguer anomaly (contours every 10 mGal) calculated using the four different methods described on the text: (a) from the lithosphere structure obtained combining elevation and geoid data (same figure than Fig. 5); (b) filtering the measured Bouguer anomaly using a Gaussian boxcar filter with a wavelength of 500 km; (c) from a lithosphere structure obtained assuming Airy crustal isostasy; (d) from a lithosphere structure obtained assuming lithosphere isostasy under pure shear deformation. Shading indicates elevation.

Figure S2. Residual Bouguer anomaly (contours every 10 mGal) resulting from subtracting the regional gravity (Fig. S1) to the measured (Fig. 3a). Shading indicates elevation.

Please note: Wiley-Blackwell are not responsible for the content or functionality of any supporting materials supplied by the authors. Any queries (other than missing material) should be directed to the corresponding author for the article.